POLITECNICO DI TORINO

Bachelor's Degree Course in Automotive Engineering

Bachelor's Degree Thesis

# Inclusion of TEPs to optimize the debonding of structural adhesives

A multiscale modelling approach to analyze how different TEPs contents affect the adhesive mechanical properties

**Supervisor:**

prof. Raffaele Ciardiello

**Co-supervisor:**

prof. Alberto Ciampaglia

**Candidate:**

Carlo Vittorio Colucci

July 2023

*I express my gratitude to my parents, my girlfriend Asia and my brother Mhamad, who are the mentors of my success.*

*Thank you to my closest friends, for always being on my side, and to my professors, especially to the beloved Elvio Bonisoli, for having made me so much passionate of their subjects, acquiring the right engineering mindset.*

## Abstract

This research aims to optimize the debonding of structural adhesives, for automotive applications, by the inclusion of TEPs (thermally expandable particles). The multiscale modelling technique was adopted to characterize TEPs mechanical properties and to simulate how different TEPs contents affect the structural behaviour of the adhesive. Retrieving the optimal percentage of inclusion particles in the adhesive matrix is an important step to reach the best trade-off between the preservation of good structural properties and a facilitated adhesive debonding.


## Acronyms

| | |
|---|---|
| **CT** | computerized tomography |
| **E** | elasticity / Young modulus |
| **ELV** | end-life vehicles |
| **FE** | Finite element |
| **K** | hardening modulus |
| **n** | hardening exponent |
| **RSF** | residual stiffness factor |
| **RVE** | representative volume element |
| **TEP** | thermally expandible particle |
| **US** | ultimate strain / strength |
| **Y** | yelding |

# Table of Contents

# 1. Structural adhesives

The need of reducing weight and to improve the mechanical performances of the vehicle led to prompted research of new technologies. The joining of the vehicles structural components is one of the engaged fields.

Classical techniques adopted for this kind of joining are:

- Fusion welding: usage limited to steels, with its alloys, and to aluminium alloys. Cheap technique which presents, around the joint, a uniform stress distribution, but an altered metal microstructure due to the high heat input;

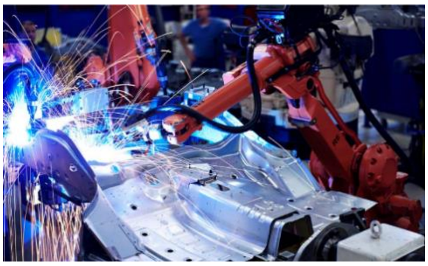

*Figure 1: Fusion welding adoption for the chassis mounting*

- Friction element welding: usage extended to the joining of non-ferrous materials with ferrous ones (such as fibre composite), but with the addition of weight due to the metal joint used. Non-uniform stress distribution around the joint, due to the discontinuity that it creates, but the low heat input generated by the metal plastic deformation, during the process, doesn't alter the metal microstructure;

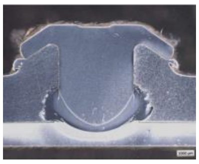

*Figure 2: Friction element welding*

- Mechanical joining: possibility of joining whatever material, but expensive and heavy solution.

*Figure 3: Mechanical joining*

A very effective alternative to these joining techniques is the adhesive: epoxy resin (thermoset polymer) with heavy structural properties, lightweight if compared to some of the previous listed joining solutions. The adhesive ensures a uniform stress transfer from a work piece to the other, allowing also eventual thermal deformations of the base materials.

## 1.1. Adhesive

There are several kinds of adhesive matrices, differing on chemical composition, which determines their structural properties and so their final application. The adhesive matrix used for this study is the SikaPower®-1277, a two-component structural epoxy adhesive. It can be applied to join aluminium and steel metal sheets, but also carbon fibre laminates, all applications where high mechanical and impact properties are required.

## 1.2. Adhesive mechanical properties characterization

The adhesive producer provides a datasheet [1] (see Appendix 1) with some of the most characterizing material properties. By the way, for the purposes of this study, some of these were computed again for a better accuracy, by a specimen tensile test, following the ISO standard procedure.

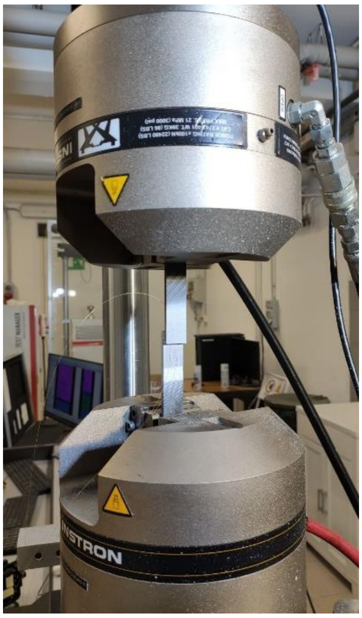


*Figure 4: Tensile test apparatus*

The specimen was composed by two composite sheets, bonded together by the concerned adhesive, through a lap joint:

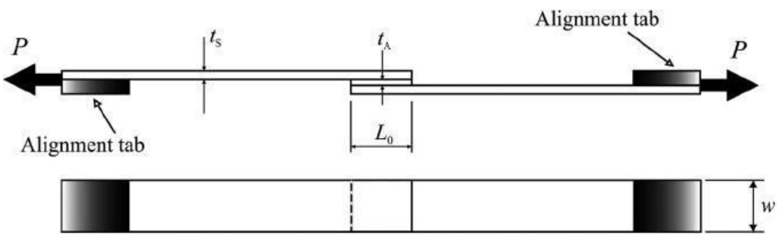


*Figure 5: Specimen design characteristics*

$$L_0 = 26.289mm; \quad S_0 = w \cdot t_A = 16.8mm^2.$$

As Figure 5 shows, the adhesive is subjected only to shear stresses. This should be the only possible working condition for this kind of joining technique, due to its weakness to withstand peel stresses.

The tensile test data were analysed by Matlab, aiming to retrieve the following parameters:

a) Young modulus ($E$);

b) Yelding strain and stress ($\varepsilon_Y, \sigma_Y$);

c) Ultimate strain and tensile strength ($\varepsilon_{US}, \sigma_m$);

d) Hardening exponent and modulus ($n, K$).

The resulting tensile test by laboratory activities is the following:

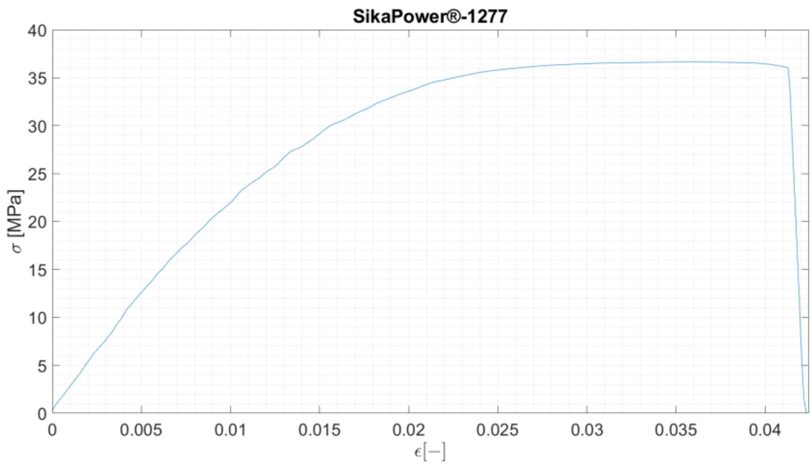


*Figure 6: Adhesive tensile test result*

The mathematical expression, well representing the trend of this tensile test, follows:

$$\begin{cases} \sigma = E \cdot \varepsilon; \quad \varepsilon \in \{0, \varepsilon_Y\} \quad (1) \\ \sigma = \sigma_Y + K \cdot \varepsilon^n; \quad \varepsilon \in \{\varepsilon_Y, \varepsilon_{US}\} \quad (2) \end{cases}$$

The curve plastic range can be approximated by different laws, but the power law is the simplest one and suits for the software implementation, as shown soon.

a) The standard EN ISO 527-2 [2] states that the value of the elasticity modulus is measured as the average slope of the tensile test curve, between elastic strains of 0.05% and 0.25%:

$$E_{matrix} = \frac{\sigma_{0.25\%} - \sigma_{0.05\%}}{\varepsilon_{0.25\%} - \varepsilon_{0.05\%}} = 2486.6MPa.$$

b) Starting from the strains in the tensile test, it's possible to retrieve the yelding point as follows:

$$\varepsilon = \varepsilon_{elastic} + \varepsilon_{plastic} = \frac{\sigma}{E_{matrix}} + \varepsilon_{plastic} \rightarrow \varepsilon_{plastic} = \varepsilon - \frac{\sigma}{E_{matrix}}$$

The array of numbers returned by this equation corresponds only to the plastic deformation and can be split in two parts, characterized by:

- The starting values very close to zero, or at least negative, within the elastic region;
- Positive values, within the plastic region.

Thus, checking what is the first positive number, the index of the yelding point is determined. The final step consists in associating to this index the relative yelding strain and stress:

$$\varepsilon_Y = 0.54\%; \quad \sigma_Y = 13.5134MPa.$$

c) The values of the tensile strength of the ultimate strain correspond to the maximum values of the two relative arrays, correspondingly:

$$\varepsilon_{US} = 4.25\%; \quad \sigma_m = 36.6347MPa.$$

d) Eq. 2 is the starting point to retrieve, firstly, the plastic stress, and then the hardening parameters:

$$\sigma_{plastic} \equiv \sigma(\varepsilon_{plastic}) = K \cdot \varepsilon^n \quad (3)$$

$$\sigma_{plastic} = \sigma - \sigma_Y \quad (4)$$

Once retrieved the plastic stresses, a minimization technique is adopted to optimize the fit of the analytical curve on the real one. The hardening modulus and exponent obtained follow:

$$K = 107.1682MPa; \quad n = 0.3735.$$

Finally, having defined all the structural parameters, it's possible to graphically represent the analytical model:

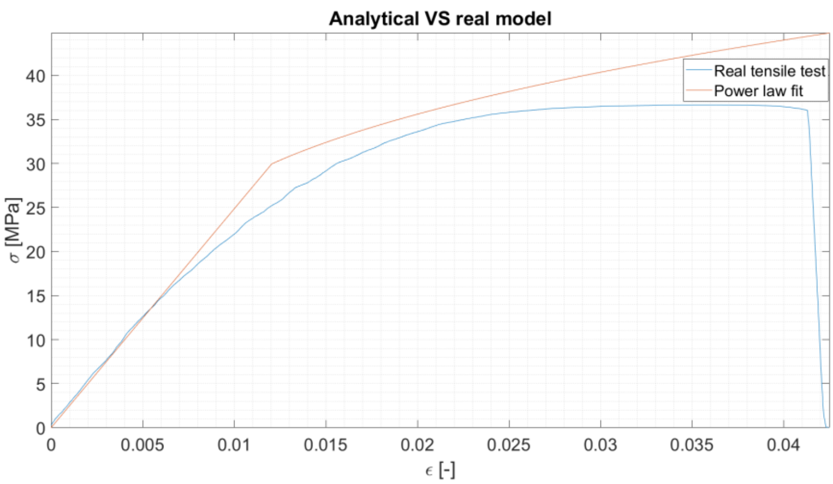


*Figure 7: Analytical model of the real tensile test*

# 2. Need of debonding

Nowadays, the environmental health care is one of the main focuses. The European Parliament established different guidelines that vehicles producers must follow to ensure their products to be the most sustainable possible. One important field concerning sustainability is the recyclability and/or reusability of the vehicle, with its components, and the Directive 2000/53/EC [3] on end-life vehicles (ELV) did set clear targets to be reached within next years. The key steps in recent years, with regard to this EU policy, are the following:

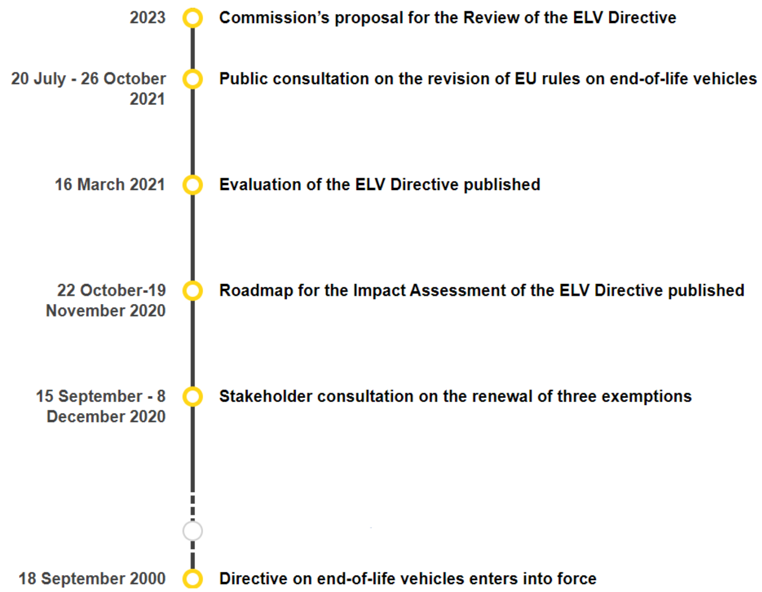


*Figure 8: Key dates of the directive on ELV*

The Directive 2000/53/EC, as reported on the official European Union website [4], sets out measures to prevent and limit waste from end-of-life vehicles and their components by ensuring their reuse, recycle and recovery. It also aims to improve the environmental performance of all economic operators involved in the life-cycle of the vehicles.

Producers, when designing and producing their products, must ensure that new vehicles are:

- reusable and/or recyclable to a minimum of 85% by weight per vehicle
- reusable and/or recoverable to a minimum of 95% by weight per vehicle.

To satisfy these requirements new solutions in different fields must be adopted. Joining of structural components is one of the concerned fields: the dismounting of vehicles parts must be guaranteed to allow their correct reuse and/or recover.

As previously highlighted, the adoption of adhesives as a joining system is convenient, but the de-bonding phase is still quite tricky, especially if reusage of the surfaces must be guaranteed. An innovative technique able of solving quite well these troubles is the inclusion of thermally expandible particles (TEPs) within the adhesive matrix.

## 2.1. TEPs

A single particle is composed of liquid hydrocarbon contained within a shell made of a co-polymeric material. The shell composition isn't exactly known, but two main monomers may be the poly vinyl chloride (PVC) and the acrilonitrile-butadiene-stirene, with the former one increasing the overall permanent deformation, as shown by Dobrotă et al [5].

When heat is provided to the adhesive, TEPs start to expand, reaching debonding at a temperature strictly dependent on the particles volume content and on the matrix adopted. The two main mechanisms concerned to the TEPs expansion are: softening of the shell and gasification of the hydrocarbon.

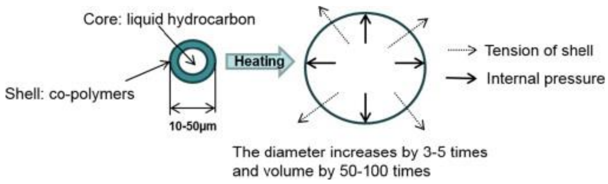


*Figure 9: TEPs structure and expansion*

Jorge Veloso [6] demonstrated that, for a 15% TEPs content, 143.3 °C is the temperature for an affective debonding of a SikaPower adhesive, like the one whose behaviour is investigated in this study.

Heat is provided by means of an electromagnetic induction coil, which allows for a fast and localised heat input.

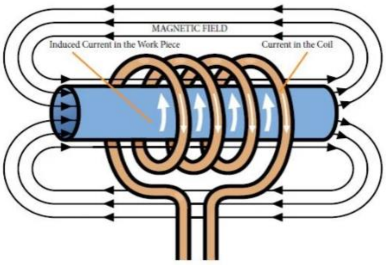


*Figure 10: Electromagnetic induction coil*

TEPs significantly affect the mechanical properties of the adhesive and it's very important to predict how the material behaviour changes with different microspheres contents, that is the main goal of this study.

## 2.2. TEPs characterization

An important step is the characterization of the mechanical properties of the microspheres and of the volumetric space they occupy within the matrix, to later analyse how these inclusions affect the overall mechanical behaviour of the adhesive.

The name of the analysed microspheres is Expancel® 093 DU 120. The producer provides only a few particles parameters useful for the current analysis [7] (see Appendix 2), such as density. By the way, some parameters needed to be recomputed more accurately, while others needed to be retrieved from the outset.

The dimensions distribution of the particles was characterized by a CT scan of a specimen charged with TEPs, whose data were analysed by Matlab. This non-destructive examination is one of the most accurate and efficient ways to characterise particles diameters at such a small length scale.

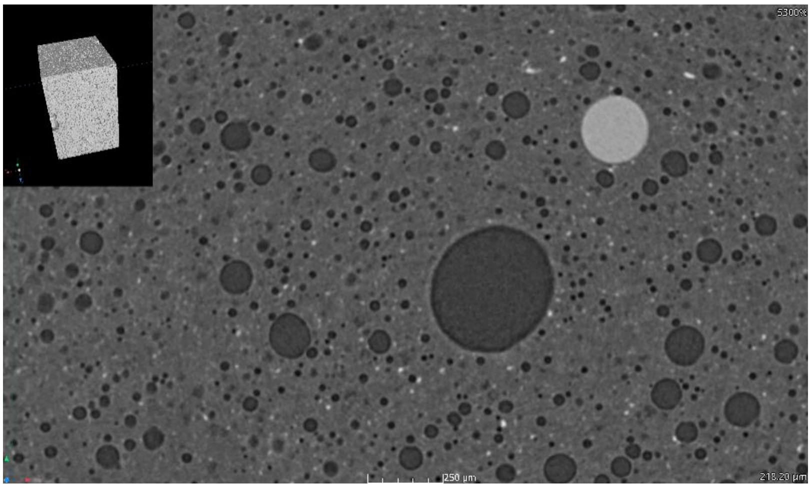

*Figure 11: Specimen CT scan*

Starting from the raw data collected, a data cleansing is necessary to avoid improper results. From statistical theory, it's known that the 98% of all the data are beneath the upper limit diameter defined as: $d_{max} = \mu + 3 \cdot s$, where µ is the mean diameter and $s$ is the standard deviation scalar, retrieved by a first data analysis of the whole data set.

The main parameters of the cleansed statistical distribution follow:

| **Mean diameter [µm]** | **Standard deviation [µm]** | **Minimum diameter [µm]** | **Maximum diameter [µm]** |
|---|---|---|---|
| 44.55 | 19.48 | 19.66 | 130.58 |

*Table 1: Statistical distribution parameters*

Starting from these parameters, this is the resulting statistical distribution:

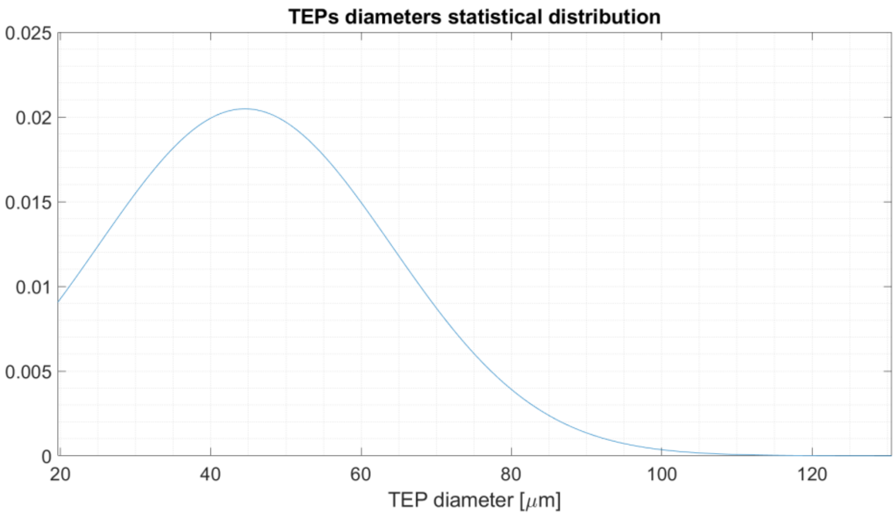


*Figure 12: TEPs diameters statistical distribution*

The last parameter to retrieve, and also the trickiest one, is the TEPs Young Modulus, but in order to do this, it is necessary to adopt a new technique called multiscale modelling.

# 3. Multiscale modelling

To describe what is the material reaction to a specific load, there are two different approaches:

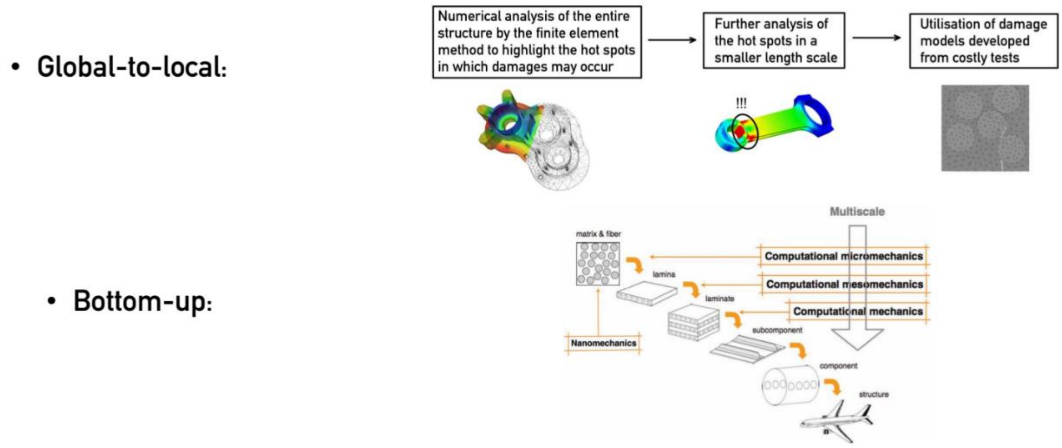


*Figure 13: Comparison between different analyses approaches*

The most used one is the bottom-up [8], which exploits numerical simulations starting from a microscopic length scale, avoiding a number of costly mechanical tests. From now on the focus will be set on this approach.

## 3.1. Composite material

The subject of this analysis is a composite material, defined as the assembly of two or more materials, with the matrix ensuring cohesion and orientation of the load. In this case, the second phase (TEPs), instead of being added to improve the final assembly mechanical properties, is added to improve the debonding of the matrix (SikaPower®-1277) when required, as previously described.

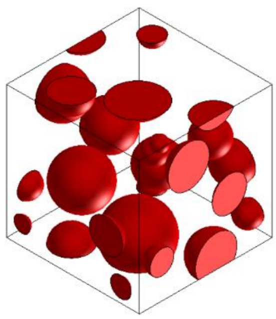

*Figure 14: Composite sample*

## 3.2. Digimat-FE

The multiscale modelling software adopted for this study purposes is Digimat-FE. This software enables to predict the behaviour of heterogeneous and/or anisotropic materials, basing on the finite element homogenization module of Digimat [9]. A representative volume element of the composite is initially set up and then meshed, solved and post-processed entirely within Digimat-FE.

## 3.3. Main parameters

To run a simulation, it's necessary to set the different phases parameters and microstructures and then, the RVE dimension with the mechanical load applied and the failure model.

Not all the parameters characterizing the following listed sections are known from the outset, but they can all be computed mainly through reverse engineering, as later explained in Section 4.

a) Materials:

All the mechanical parameters retrieved until now must be set in this section.

- Matrix - SikaPower®-1277:

| | |
|---|---|
| **Young modulus [MPa]** | 2486.6 |
| **Yelding stress [MPa]** | 13.5134 |
| **Ultimate strength [MPa]** | 36.6347 |
| **Hardening modulus [MPa]** | 107.1682 |
| **Yelding strain [%]** | 0.54 |
| **Ultimate strain [%]** | 4.25 |
| **Hardening exponent [-]** | 0.3735 |
| **Poisson ratio [-]** | 0.4 |
| **Density [kg/m^3]** | 1100 |

*Table 2: Matrix structural properties*

The matrix behaviour simulated by Digimat with these parameters is:

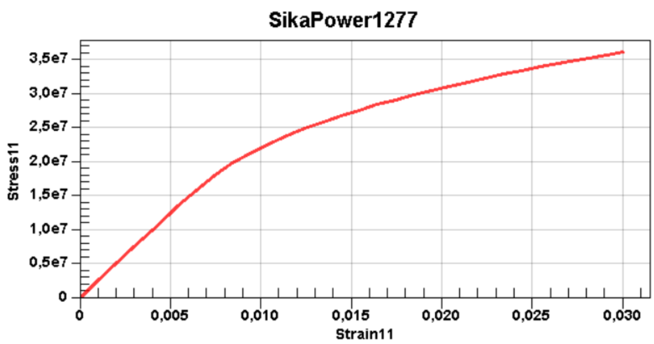


*Figure 15: Digimat matrix simulation*

As it's possible to notice comparing this result with the original one from the tensile test carried out, it's evident the similarity between the two curves, as expected.

- TEPs - Expancel®093 DU 120:

It's worth it to highlight that the Poisson ratio is unknown but, starting from the microspheres shell material, with its constituent co-polymer Poisson ratio of 0.4, the TEPs one can be considered the same. On the other hand, the Young modulus, as previously said, is unknown too, but it's possible to retrieve it by Digimat simulations, as shown later on (Section 5).

The parameters known until now are the density and the Poisson ratio:

$\rho_{TEPs} = 6.5\ kg/m^3$; $\nu_{TEPs} = 0.4$.

b) Microstructure:

The only microstructure to be set with its proper parameters is the inclusion one:

- The volume fraction considered is dependent on the goal of the simulation carried out;
- The shape of the TEPs is set spherical, that is quite a good approximation of the realty;
- The data about the distribution of the microspheres dimensions were retrieved in Section 2.2.

c) RVE:

The RVE size is initially suggested by Digimat ($222.751^3\ \mu m^3$) and it can be a good starting point to carry out simulations to find initial needed parameters, such as the TEPs E-modulus. After all the mechanical properties are established, it's necessary to conduct a study about what RVE size best simulates the realty, as it will be shown later (Section 6).

d) Failure:

The failure indicator is relevant for the simulation since it aims to prevent when the material will fail and how it will. Two different models are tested, with results reported in Section 7.

e) Loadings:

The loading type may be both the strain and the stress along the principal direction. The value selected corresponds to the maximum one the simulated material is expected to withstand until fracture.

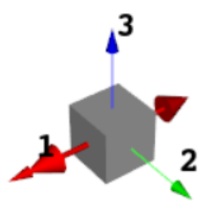


*Figure 16: Load orientation*

# 4. Adhesive charged with TEPs

Another tensile test in laboratory was carried out on a SikaPower®-1277 adhesive matrix filled at the 17% with Expancel® 093 DU 120.

The characterization procedure is the same as explained in Section 1.2 but, in this case, only the elasticity modulus and the ultimate strain are researched:

$$E_{composite} = \frac{\sigma_{0.25\%} - \sigma_{0.05\%}}{\varepsilon_{0.25\%} - \varepsilon_{0.05\%}} = 2107MPa; \quad \varepsilon_{US} = 1.01\%.$$

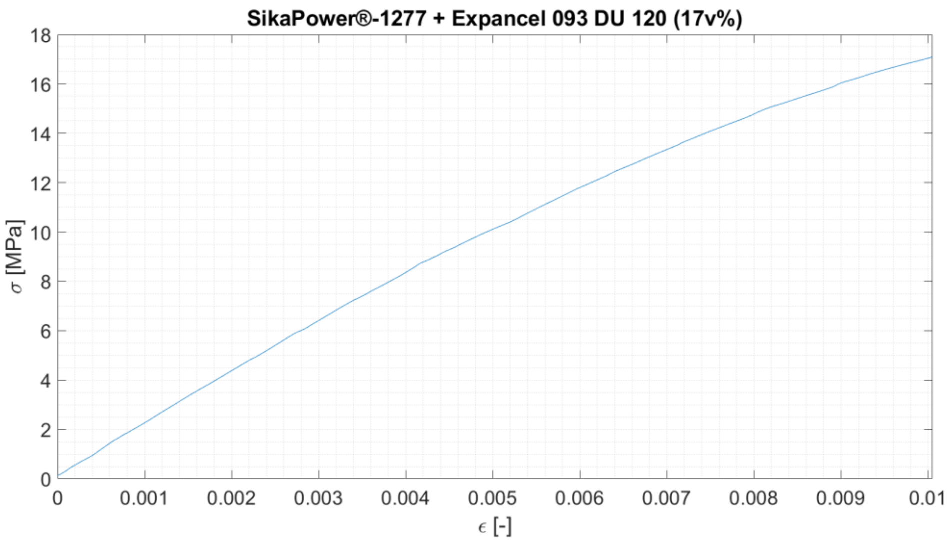


*Figure 17: Composite tensile test*

This composite test will be the reference for the next analyses, because it represents the real model that the simulation results must be able to emulate. Thus, a reverse engineering procedure will be adopted: start from the result to obtain information about the system.

# 5. TEPs Young modulus characterization

The tests to retrieve the TEPs E-modulus start from a blank sheet, because no information about a hypothetical value is available. The first choice is a very low tentative value, considering that only the TEP shell is "rigid", while the infill is liquid:

$$E^0_{TEPs} = 20MPa.$$

A trial-and-error approach is adopted: simulations with different TEPs E-modulus are undertaken to find a correspondence between the simulated composite Young modulus and the reference one previously characterized ($E_{TEPs} = 2107MPa$). Starting from the simulation results, the equation used to compute the E-modulus is the same used in Section 1.2:

$$E_{composite} = \frac{\sigma_{0.25\%} - \sigma_{0.05\%}}{\varepsilon_{0.25\%} - \varepsilon_{0.05\%}}$$

Since these required strain values aren't precisely available in the results set of points, the closest values available are chosen.

Starting from the first tentative modulus, 6 further simulations are necessary to reach a fine result:

1) $E^1_{TEPs} = 200MPa;$
2) $E^2_{TEPs} = 2000MPa;$
3) $E^3_{TEPs} = 1766MPa;$
4) $E^4_{TEPs} = 1300MPa;$
5) $E^5_{TEPs} = 800MPa;$
6) $E^6_{TEPs} = 850MPa.$

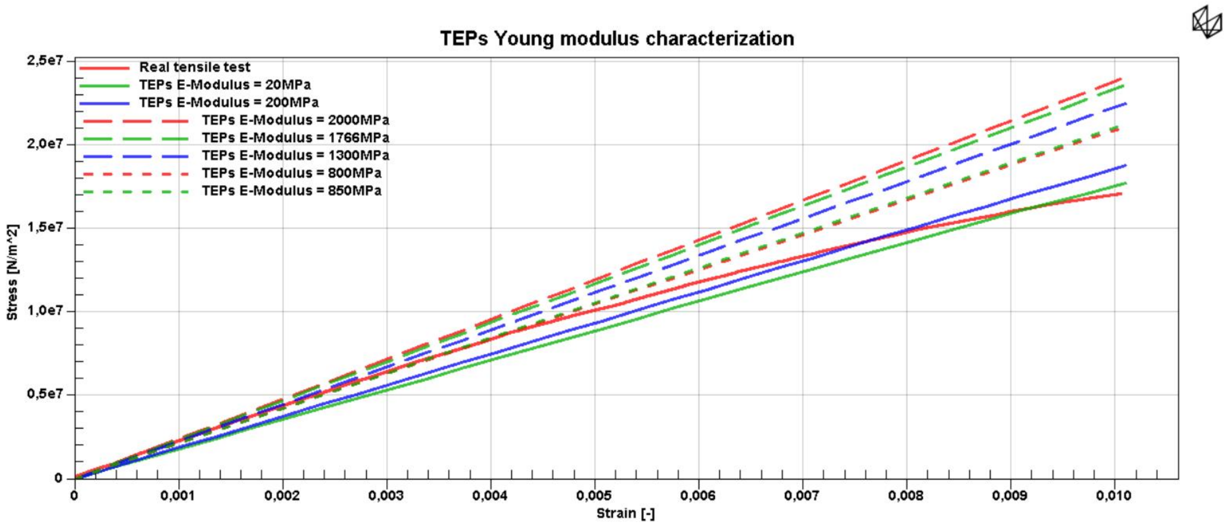


*Figure 18: TEPs E-modulus characterization*

With $E_{TEPs} = 850MPa$, the simulated composite E-modulus computed is:

$$E_{composite} = \frac{4.9851 - 1.4255}{2.3658 \cdot 10^{-3} - 6.7652 \cdot 10^{-3}} MPa = 2107.2 MPa.$$

Once retrieved the optimal starting modulus, it is necessary to validate it. To do this, simulations with different RVE sizes are carried out. A different size corresponds to a different resolution of the result: a bigger representative volume is expected to better simulate the realty, due to the major space that the statistical distribution can exploit to reach the requirements imposed by the user. For each RVE size, 3 different RVEs are generated and simulated, to obtain an accurate result for each size.

Each simulation is approached as previously done for the research of the starting TEPs E-modulus: trial-and-error until the correct value isn't reached.

| TEPs Young Modulus [MPa] | *RVE side: 200.476μm* | *RVE side: 222.751μm* | *RVE side: 245.026μm* | *RVE side: 267.301μm* |
|---|---|---|---|---|
| *Structure 1* | 845 | 857.5 | 847.5 | 857 |
| *Structure 2* | 817.5 | 882.5 | 848.5 | 840 |
| *Structure 3* | 927.5 | 800 | 810 | 905 |
| *Mean value* | *863* | *847* | *835* | *867* |

*Table 3: Simulations for the TEPs E-modulus validation*

Different simulations are discarded during the process, because not all the RVEs generated are able to precisely satisfy the requirements on the TEPs volume content, leading to wrong results.

Computing the mean value of these different moduli, the validated value of the TEPs Young Modulus is:

$$E_{TEPs} = 853.1 MPa.$$

This value completes all the materials mechanical properties required to run an affordable simulation.

# 6. Optimization of the RVE size

As explained in the previous Section, RVEs of different dimensions may correspond to different quality results. To optimize this parameter, 4 different simulations are undertaken with the same RVE dimensions used for the tests in the previous Section. The TEPs volume content is fixed, as usual, to the reference value of 17% and only RVEs of different dimensions with a TEPs content within the range of $17 \mp 0.25\%$ are adopted. For each simulation the resulting composite E-modulus is computed and the deviation with respect to the real value is considered to compare the different results:

| | **RVE side: 200.476µm** | **RVE side: 222.751µm** | **RVE side: 245.026µm** | **RVE side: 267.301µm** |
|---|---|---|---|---|
| Volume content [%] | 17.0095 | 17.0769 | 17.2177 | 17.192 |
| Composite Young modulus [MPa] | 2128 | 2100 | 2098 | 2111 |
| Deviation [MPa] | 28 | 7 | 9 | 4 |
| RVE | 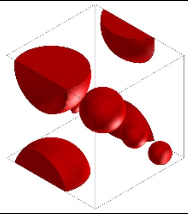 | 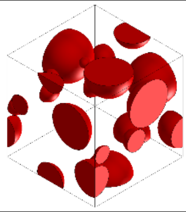 | 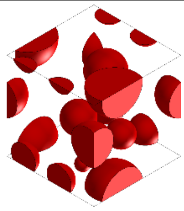 | 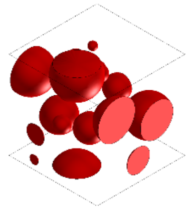 |

*Table 4: RVE size optimization*

The RVE size with the smallest deviation is the biggest one: $267.301^3\ \mu m^3$. This result agrees with the previous considerations and it will be the dimension used for the simulations from now on.

# 7. Failure indicator set up

Two different models are tested, both at matrix level: Von Mises and Stress Component.

The Von Mises criterion [10] collects one input and returns 1 output:

- Input:

Von Mises strength: $S = 36.6347MPa$.

- Output:

Failure indicator:

$f_A - \frac{J_2}{S_2}$ with $J_2 = [(\sigma_{11} - \sigma_{22})^2 + (\sigma_{22} - \sigma_{33})^2 + (\sigma_{33} - \sigma_{11})^2] + 3 \cdot [\sigma_{12}^2 + \sigma_{23}^2 + \sigma_{13}^2]$

The Stress Component [11] is a model convenient for its usage simplicity and effectiveness. It requires 3 inputs and returns 2 outputs:

- Input:

1. Component of the stress tensor used: in this case there is only the presence of a uniaxial stress along the principal direction;
2. Tensile strength of the matrix: $X_t = 36.6347MPa$;
3. Compressive strength of the matrix: the value is arbitrary chosen much higher than the tensile strength one ($X_c = 1000MPa$), in order to avoid misleading errors due to eventually compressive stresses, even if these may not occur.

- Output:

The failure indicator is computed in the principal axes of the stress tensor, thus, only the diagonal terms of the tensor are different from zero. In this case, the eigen values are ordered as follows: $\sigma_{11} \geq \sigma_{22} \geq \sigma_{33}$.

1. Tensile failure indicator:

$f_A = F_A(\sigma)$ with $F_A(\sigma) = \frac{\sigma_1}{X_t}$ if $\sigma_1 > 0$, 0 otherwise;

2. Compressive failure indicator:

$f_B = F_B(\sigma)$ with $F_B(\sigma) = -\frac{\sigma_3}{X_c}$ if $\sigma_3 < 0$, 0 otherwise.

Failure is encountered if (at least) one of these two indicators reaches the critical value of 1.

An important parameter determining the damage behaviour of the material is the Residual stiffness factor:

$$RSF = \frac{Composite\ stiffness\ after\ damage\ or\ failure}{Initial\ compoiste\ stifness}$$

To facilitate the understanding of how these two failure indicators work and of how the RSF affects the material behaviour, the strain load is extended to $\varepsilon_{US} = 0.2$.

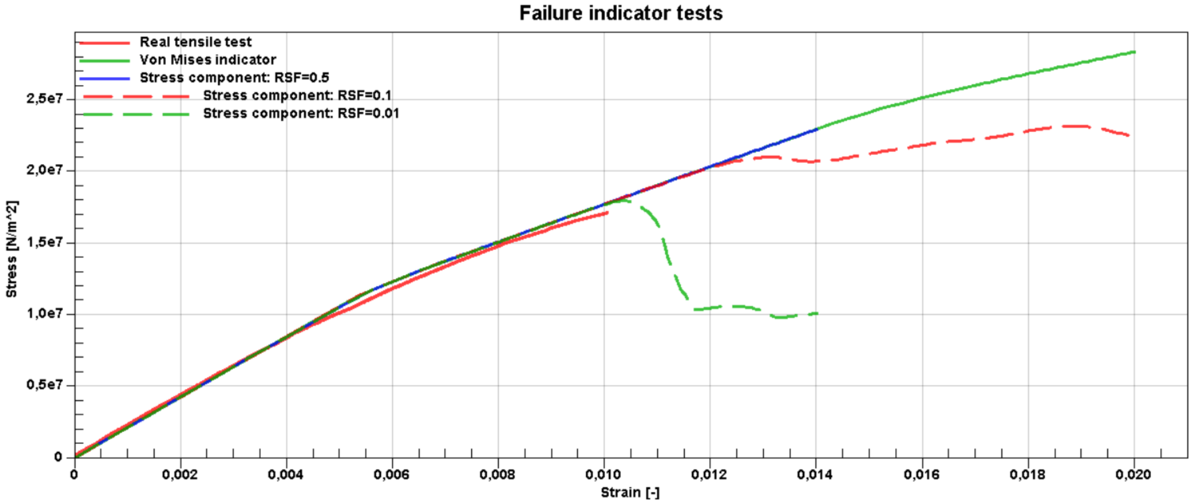


*Figure 19: Failure indicator tests*

The Von Mises model misses the fracture point, returning a non-consistent result, while the Stress Component affects the material behaviour, getting closer to the real phenomenon, especially for lower RSF values.

Thus, the failure indicator chosen is the Stress Component, selecting the lower limit of RSF available ($RSF = 0.01$). It's noteworthy the damage starting point to be very close to the real composite ultimate strain ($\varepsilon_{US} = 0.0101$), giving evidence of the simulation precision. Until strain values around 0.012, the trend follows the expected one, getting weird beyond this threshold. In order to have a better representation of the realty, the following simulations are going to be cut in the region attending this weird behaviour.

In conclusion, Digimat allows to graphically visualize the stress concentration in the different RVE points and it allows to exaggerate the strain level too, to understand how the material deforms under the applied load:

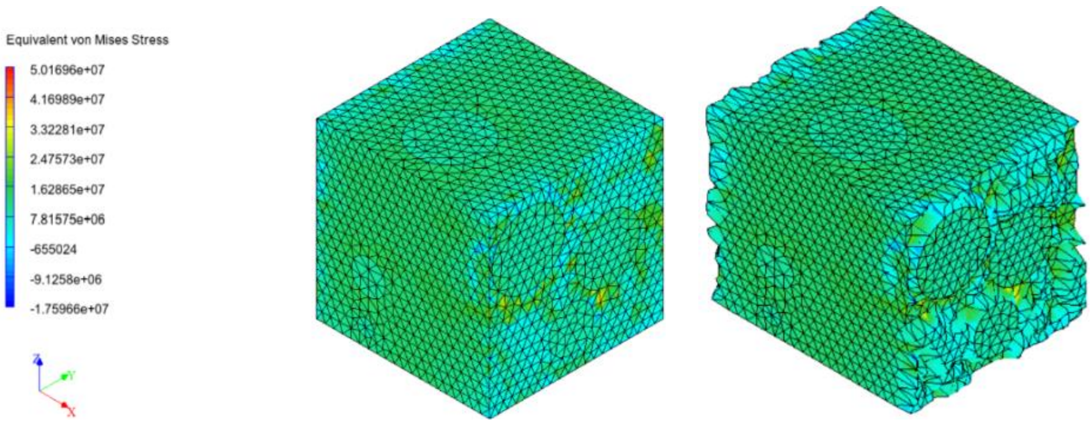


*Figure 20: Comparison between the normal stress visualization and the exaggerated strain*

# 8. Optimization of the TEPs content

Once all the needed parameters to carry out an accurate simulation have been fixed, it's possible to analyse how the different TEPs volume contents affect the material structural behaviour. Starting from the simulation with the reference volume content, 4 further simulations are undertaken. The target values of volume content are: 5%, 10%, 17%, 25%, 30%. Deviations of TEPs content, in the RVE generation, within a range of ∓0.3 are accepted.

For each simulation, the mechanical properties of the resulting composite are analysed Matlab through, computing:

a) Young modulus;

b) Tensile stress;

c) Ultimate strain;

d) Yelding stress;

e) Yelding strain.

Before showing the simulation results, a recap of the matrix mechanical properties follows:

| **TEPs volume content: 0%** | $E\ [MPa]$ | $\sigma_m\ [MPa]$ | $\varepsilon_{US}$ [%] | $\sigma_Y\ [MPa]$ | $\varepsilon_Y$ [%] |
|---|---|---|---|---|---|
| | 2486.6 | 36.6347 | 4.25 | 13.5134 | 0.54 |

<table>
<tr><td>TEPs volume content: 5.05117%</td><td colspan="3">RVE</td><td colspan="3">Stress analysis</td></tr>
<tr><td rowspan="3"></td><td colspan="3">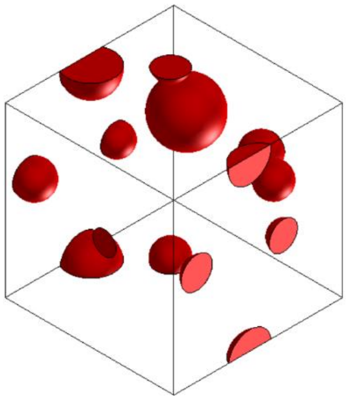</td><td colspan="2">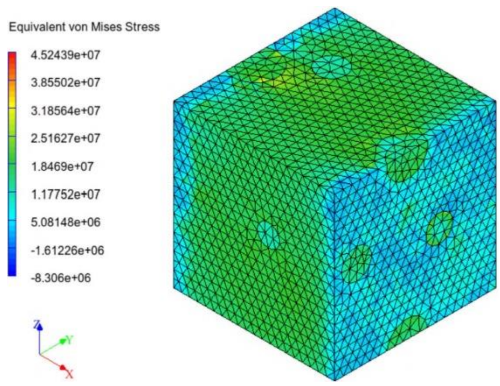
</td></tr>
<tr><td>$E\ [MPa]$</td><td>$\sigma_m\ [MPa]$</td><td>$\varepsilon_{US}$ [%]</td><td>$\sigma_Y\ [MPa]$</td><td>$\varepsilon_Y$ [%]</td></tr>
<tr><td>2369.8</td><td>21.794</td><td>1.4154</td><td>9.6518</td><td>0.4073</td></tr>
</table>

<table>
<tr><td>TEPs volume content: 9.88283%</td><td colspan="3">RVE</td><td colspan="3">Stress analysis</td></tr>
<tr><td rowspan="3"></td><td colspan="3">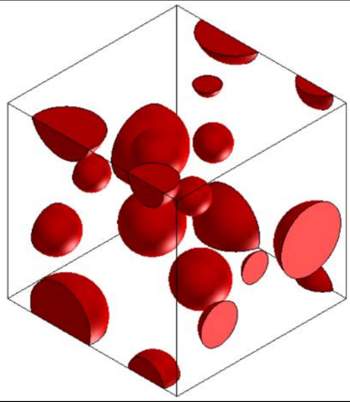</td><td colspan="3">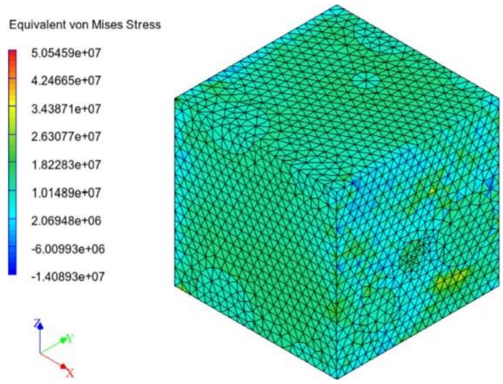
</td></tr>
<tr><td>$E\ [MPa]$</td><td>$\sigma_m\ [MPa]$</td><td colspan="2">$\varepsilon_{US}$ [%]</td><td>$\sigma_Y\ [MPa]$</td><td>$\varepsilon_Y$ [%]</td></tr>
<tr><td>2257.1</td><td>19.9</td><td colspan="2">1.2582</td><td>13.153</td><td>0.6027</td></tr>
<tr><td>TEPs volume content: 17.192%</td><td colspan="3">RVE</td><td colspan="3">Stress analysis</td></tr>
<tr><td rowspan="3"></td><td colspan="3">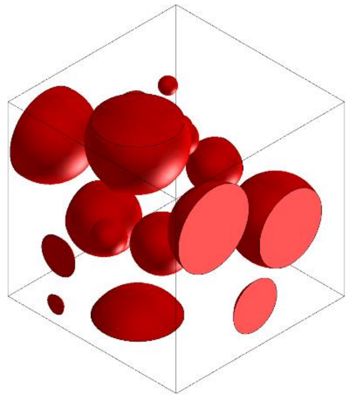</td><td colspan="3">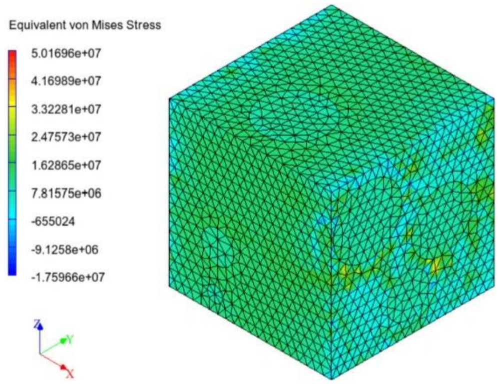
</td></tr>
<tr><td>$E\ [MPa]$</td><td>$\sigma_m\ [MPa]$</td><td colspan="2">$\varepsilon_{US}$ [%]</td><td>$\sigma_Y\ [MPa]$</td><td>$\varepsilon_Y$ [%]</td></tr>
<tr><td>2111.2</td><td>17.942</td><td colspan="2">1.1662</td><td>12.443</td><td>0.6091</td></tr>
<tr><td>TEPs volume content: 24.7883%</td><td colspan="3">RVE</td><td colspan="3">Stress analysis</td></tr>
<tr><td rowspan="2"></td><td colspan="3">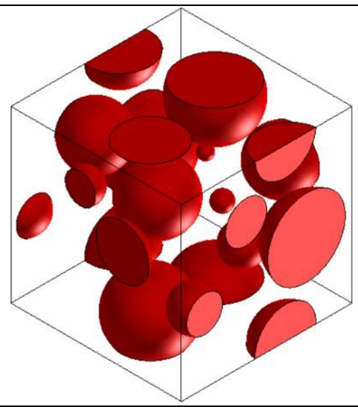</td><td colspan="3">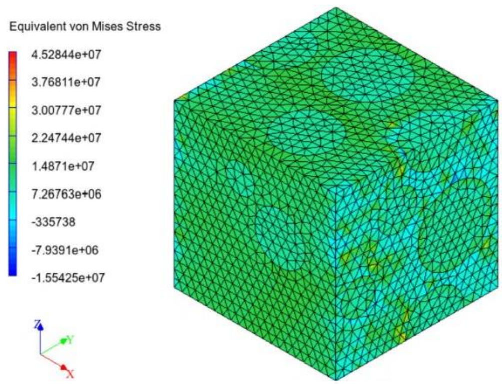
</td></tr>
<tr><td>$E\ [MPa]$</td><td>$\sigma_m\ [MPa]$</td><td colspan="2">$\varepsilon_{US}$ [%]</td><td>$\sigma_Y\ [MPa]$</td><td>$\varepsilon_Y$ [%]</td></tr>
</table>

| | | | | | |
|---|---|---|---|---|---|
| | 1946.7 | 15.229 | 1.0614 | 11.262 | 0.5908 |
| **TEPs volume content: 29.7158%** | RVE | | Stress analysis | | |
| | 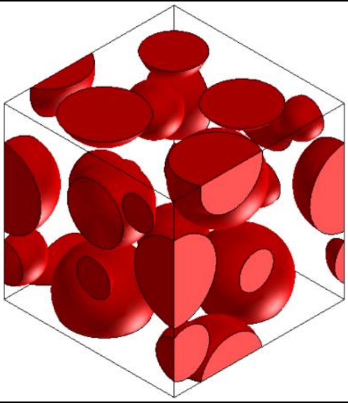 | | 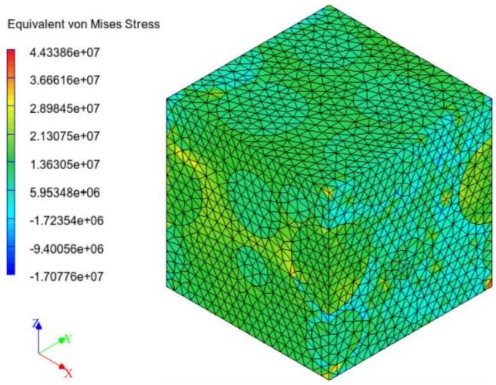 | | |
| | $E\ [MPa]$ | $\sigma_m\ [MPa]$ | $\varepsilon_{US}$ [%] | $\sigma_Y\ [MPa]$ | $\varepsilon_Y$ [%] |
| | 1856.3 | 18.015 | 1.3999 | 11.031 | 0.6091 |

*Table 5: Simulation results at different TEPs volume content*

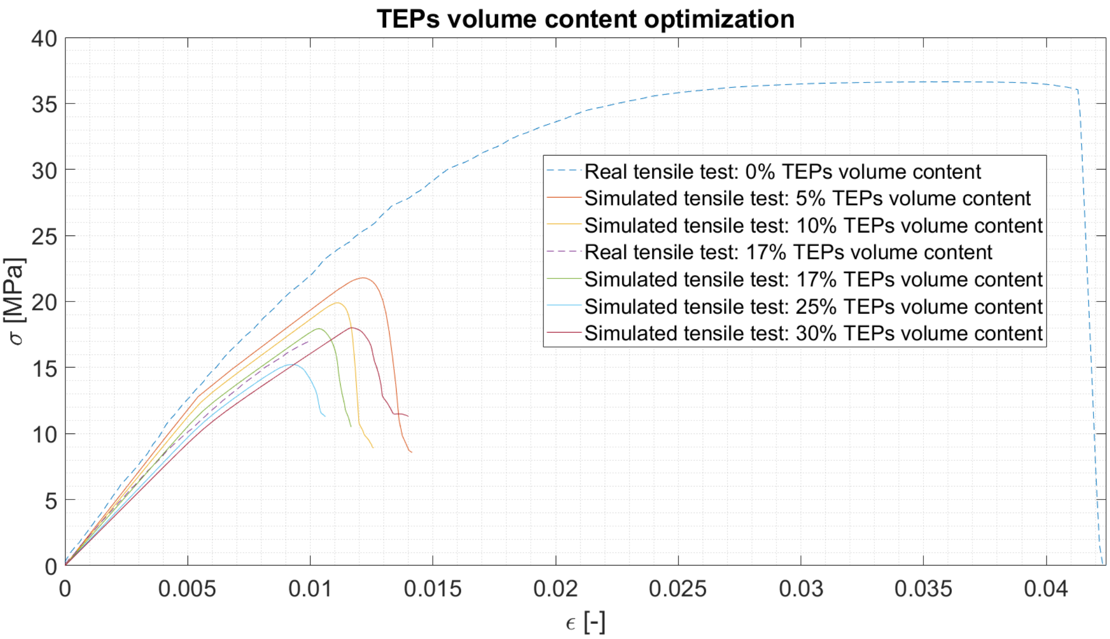


*Figure 21: Tensile test results at different TEPs volume content*

To ease the understanding in the changes of the composite mechanical properties, it may be helpful to plot them:

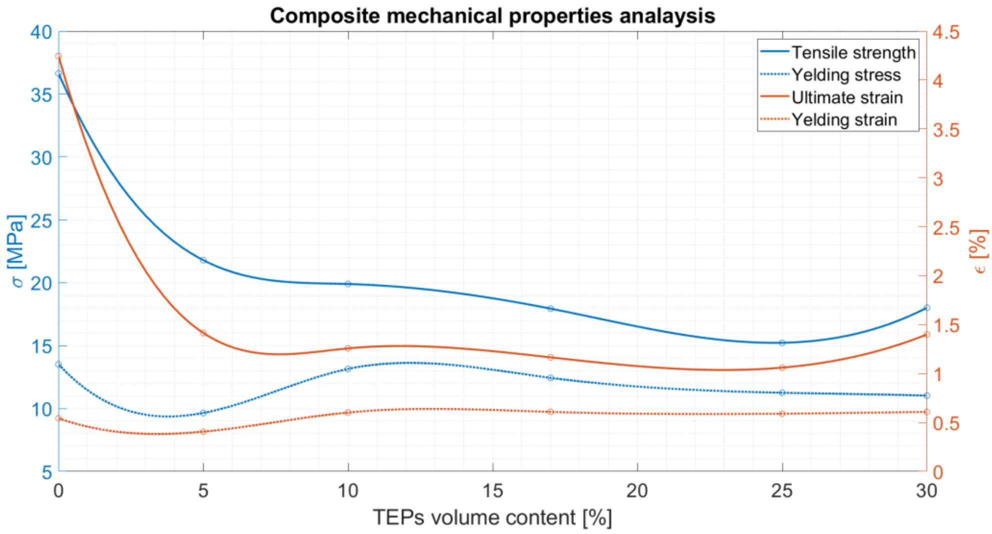


*Figure 22: Impact of TEPs volume content on the composite mechanical properties*

The difference between the ultimate strain and the yelding strain ($\varepsilon_{US} - \varepsilon_Y$), is a useful parameter to track the material ductility. The result is a decreasing trend at increasing TEPs content, highlighting a decrease in the overall composite ductility.

It's also worth it to analyse the trend of the yelding stress and strain: for higher values of TEPs content, they feature an increasing trend, resulting in a wider material elastic zone.

The Young modulus describes the stiffness of the material and its decreasing trend highlights a decreasing stiffness of the overall composite material.

In conclusion, the maximum stress and strain, that the material can withstand, are lower for higher TEPs contents, resulting in a weaker compound. This trend holds except for the last simulation, which may present a misleading result, due to the high non-linearity of the model, especially close to the neighbourhood of the maximum microspheres content that the RVE can contain.

To establish what the optimal value of TEPs volume content may be, a mechanical test alone isn't enough, a thermal analysis should accompany. By the way, this study is the halfway point towards this optimization, understanding what main changes in mechanical properties adhesive may encounter with varying TEPs contents.

# 9. Conclusions

This work has covered several steps to reach the final goal of optimizing the adhesive de-bonding under the mechanical point of view, but several other results have been obtained:

- The statistical distribution parameters of the Expancel® 093 DU 120 within an adhesive matrix were defined;
- The TEPs Young modulus value, $E_{TEPs} = 853.1 MPa$, was computed;
- The optimal RVE size ($267.301^3\ \mu m^3$) was validated;
- The failure indicator was properly tuned to obtain results the most reliable as possible;
- The mechanical properties of the composite, with different TEPs volume contents, were retrieved, understanding how the TEPs affect the mechanical behaviour of the adhesive.

Multiscale modelling adoption was crucial for the goals of this study, allowing to avoid a number of costly tests, that would have been necessary to obtain results with such a high accuracy. Nowadays tests are ever more shifted to a virtual environment, not only to save money, but also to save time and improve results accuracy.

# 10. Future work

As anticipated in Section 8, the mechanical analysis alone for the adhesive de-bonding optimization isn't enough. A thermal study may be undertaken, to understand how much the TEPs volume content encourage debonding, reaching the trade-off between an eased de-bonding and a good preservation of the adhesive mechanical properties.

Moreover, a further thermal analysis may be carried out, to understand how the material structural behaviour is affected at temperatures higher than the working condition ones. In this case, the thermomechanical analysis tool [12] by Digimat-FE may be adopted.

# BIBLIOGRAPHY


[1] URL: https://industry.sika.com/content/dam/dms/itgen/i/sikapower_-1277.pdf.

[2] M.G. Cardoso, J.E.C. Pinto, R.D.S.G. Campilho, P.J.R.O Nòvoa, F.J.G. Silva, L.D.C. Ramalho. *A new structural two-component epoxy adhesive: strength and fracture characterization.* June 2021.

[3] European parliament and council. *Directive 2000/53/EC on end-life vehicles.* September 2000.

[4] URL: https://eur-lex.europa.eu/EN/legal-content/summary/end-of-life-vehicles.html.

[5] Dan Dobrotă, Valentin Petrescu, Cristinel Sabin Dimulescu and Mihaela Oleksik. *Preparation and Characterization of Composites Materials with Rubber Matrix and with Polyvinyl Chloride Addition (PVC).* August 2020.

[6] Rui Jorge Veloso. *De-bonding on command of adhesive joints.* October 2015.

[7] URL:https://www.nouryon.com/globalassets/inriver/resources/product-overview-specification-expancel-du-global-en.pdf.

[8] J. LLorca, C. González , J. M. Molina-Aldareguía , J. Segurado , R. Seltzer , F. Sket, M. Rodríguez, S. Sádaba , R. Muñoz and L. P. Cana. *Multiscale modelling of composite materials: a roadmap towards virtual testing.* 2011.

[9] URL: https://help.hexagonmi.com/it-IT/bundle/digimat_2022.2/page/digimat_2022.2/Digimat_UG_fe/digi_ug_fe_over/TOC.General.description1.xhtml.

[10] URL: https://help.hexagonmi.com/it-IT/bundle/digimat_2022.2/page/digimat_2022.2/Digimat_UG_fe/digi_ug_fe_fail/TOC.Failure.indicators2.xhtml.

[11] URL: https://help.hexagonmi.com/it-IT/bundle/digimat_2022.2/page/digimat_2022.2/Digimat_UG_mf/digi_ug_mf_fail/TOC.Failure.indicators1.xhtml#XREF_27794_Composite.

[12] URL: https://help.hexagonmi.com/it-IT/bundle/digimat_2022.2/page/digimat_2022.2/Digimat_UG_fe/digi_ug_fe_ana/TOC.Analyses1.xhtml.

# APPENDIX 1

BUILDING TRUST

PRODUCT DATA SHEET

## SikaPower®-1277

Toughened and high impact-resistant 2-component structural adhesive

### TYPICAL PRODUCT DATA (FURTHER VALUES SEE SAFETY DATA SHEET)

| Properties | | SikaPower®-1277 (A) | SikaPower®-1277 (B) |
|---|---|---|---|
| **Chemical base** | | Epoxy | Amine |
| **Colour (CQP001-1)** | | Red | White |
| | mixed | Light red | |
| **Density** | | 1.08 g/cm³ | 1.06 g/cm³ |
| | mixed (calculated) | 1.07 g/cm³ | |
| **Mixing ratio** | A:B by volume | 2:1 | |
| | A:B by weight | 2:1 | |
| **Viscosity (CQP029-4)** | at 10 $s^{-1}$ | 430 Pa·s [A] | 100 Pa·s [A] |
| **Consistency** | | Thixotropic paste | |
| **Application temperature** | | 15 – 35 °C | |
| **Open time (CQP046-11 / ISO 4587)** | as contact adhesive | 1 hour [B, C, D] | |
| **Handling time (CQP046-11 / ISO 4587)** | | 11 hours [C, D] | |
| **Curing time (CQP046-9, ISO4587)** | time to reach 20 MPa | 24 hours [C, D] | |
| **Shore D hardness (CQP023-1 / ISO 48-4)** | | 75 [C, E] | |
| **Tensile strength (CQP543-1 / ISO 527)** | | 30 MPa [C, E] | |
| **E-Modulus (CQP543-1 / ISO 527)** | | 2 000 MPa [C, E] | |
| **Elongation at break (CQP543-1 / ISO 527)** | | 4 % [C, E] | |
| **Tensile lap-shear strength (CQP046-9 / ISO 4587)** | | 28 MPa [C, D, E] | |
| **Impact peel strength (CQP505-1 / ISO 11343)** | | 30 N/mm [C, D, E, F] | |
| **Glass transition temperature (CQP509-1 / ISO 6721)** | | 67 °C [E] | |
| **Shelf life (CQP016-1)** | cartridges | 24 months [G] | |
| | pails | 12 months [G] | |

CQP = Corporate Quality Procedure
A) tested at 20 °C
B) applied on both bonding surfaces
C) 23 °C / 50 % r. h.
D) adhesive layer: 25 x 10 x 0.3 mm / on steel
E) cured for 2 weeks at 23 °C
F) impact speed: 2 m/s
G) storage between 10 and 30 °C

### DESCRIPTION

SikaPower®-1277 is a structural 2-component epoxy adhesive, which cures at room temperature. It is designed for high strength and impact-resistant bonding of metallic substrates, like steel and aluminum, as well as of composite substrates, like GFRP and CFRP laminates. The adhesive has good non-sag properties and contains glass beads of 0.3 mm to ensure an optimal bonding thickness.

### PRODUCT BENEFITS

- High structural and high impact-resistant properties
- Contains anti-corrosion agents
- Contains glass beads to ensure an optimal bonding thickness
- Does not contain solvents or PVC
- Cures at room temperature
- Accelerated curing and higher mechanical strength with heat

### AREAS OF APPLICATION

SikaPower®-1277 is suitable for structural bonding applications in transportation and general industry. It can also be used for repair applications in combination with spot welding, riveting or clinching. The product is applied as contact adhesive (2-side application). In case of single bead application contact Sika. This product is suitable for professional experienced users only. Test with actual substrates and conditions have to be performed to ensure adhesion and material compatibility.

## CURE MECHANISM
SikaPower®-1277 cures by chemical reaction of the two components at room temperature. The cure rate is accelerated and the final glass transition temperature, as well as the tensile and shear strengths, may be significantly increased at higher curing temperatures. The following table shows typical lap-shear strengths reached after different curing times and temperatures.

| Temperature | Time | Strength |
|---|---|---|
| 23 °C | 24 hours | 20 MPa |
| 60 °C | 60 minutes | 10 MPa |
| 80 °C | 30 minutes | 15 MPa |

Table 1: Typical lap-shear strength development at different curing conditions (strength tested at 23 °C)

## CHEMICAL RESISTANCE
In view of potential chemical or thermal exposure, it is required to conduct a project related testing.

## METHOD OF APPLICATION
### Surface Preparation
Surfaces must be clean, dry and free from grease, oil and dust. Surface treatment depends on the specific nature of the substrates and is crucial for a long lasting bond. All pretreatment steps must be confirmed by preliminary tests on original substrates considering specific conditions in the assembly process.

### Application
SikaPower®-1277 is dispensed from dual cartridges with adequate piston guns or from pails with 2-component equipment. If dispensed out of equipment, the mixer needs to be tailored for the specific application.
Cartridge use: Extrude adhesive without mixer to equalize the filling levels. Attach the mixer and dispose the first few cm of the bead prior to the application.
Apply the adhesive on both bonding surfaces and use a spatula to spread it. Join the parts within the open time of 1 hour. If the product is used with a single bead contact Sika prior to the application. The mixer open time is 30 minutes.

### Removal
Uncured SikaPower®-1277 can be removed from tools and equipment with Sika® Remover-208 or another suitable solvent. Once cured, the material can only be removed mechanically. Hands and exposed skin have to be washed immediately using hand wipes such as Sika® Cleaner-350 H or a suitable industrial hand cleaner and water. Do not use solvents on skin!

## STORAGE CONDITIONS
SikaPower®-1277 has to be kept between 10 °C and 30 °C in a dry place. Do not expose to direct sunlight or frost. After opening of the packaging, the contents have to be protected against humidity.

## FURTHER INFORMATION
The information herein is offered for general guidance only. Advice on specific applications is available on request from the Technical Department of Sika Industry. Copies of the following publications are available on request:
- Safety Data Sheets

## PACKAGING INFORMATION
SikaPower®-1277 (A+B)

| | |
|---|---|
| Dual cartridge | 400 ml |
| Mixer: Sulzer MixPac™ MFQ 08-24T | |

## BASIS OF PRODUCT DATA
All technical data stated in this document are based on laboratory tests. Actual measured data may vary due to circumstances beyond our control.

## HEALTH AND SAFETY INFORMATION
User must read the most recent corresponding Safety Data Sheets (SDS) before using any products. The SDS provides information and advice on the safe handling, storage and disposal of chemical products and contains physical, ecological, toxicological and other safety-related data.

## DISCLAIMER
The information, and, in particular, the recommendations relating to the application and end-use of Sika products, are given in good faith based on Sika's current knowledge and experience of the products when properly stored, handled and applied under normal conditions in accordance with Sika's recommendations. In practice, the differences in materials, substrates and actual site conditions are such that no warranty in respect of merchantability or of fitness for a particular purpose, nor any liability arising out of any legal relationship whatsoever, can be inferred either from this information, or from any written recommendations, or from any other advice offered. The user of the product must test the product's suitability for the intended application and purpose. Sika reserves the right to change the properties of its products. The proprietary rights of third parties must be observed. All orders are accepted subject to our current terms of sale and delivery. Users must always refer to the most recent issue of the local Product Data Sheet for the product concerned, copies of which will be supplied on request.

# APPENDIX 2

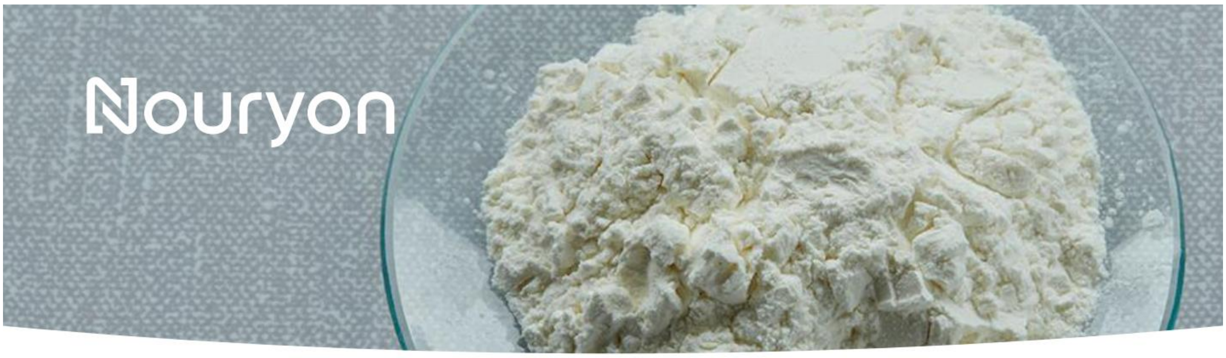


## Product specification
## Expancel® DU Microspheres

| Expancel® grade | Thermomechanical Analysis (1) Tmax °C | Tstart °C | Density kg/m³ | Particle size D(0.5) (2) µm | Solvent resistance (3) |
|---|---|---|---|---|---|
| 031 DU 40 | 118–133 | 80–95 | ≤ 12 | 10–16 | 3 |
| 053 DU 40 | 136–144 | 95–102 | ≤ 20 | 10–16 | 3 |
| 051 DU 40 | 142–151 | 105–110 | ≤ 25 | 9–15 | 4 |
| 043 DU 80 | 144–164 | 94–114 | ≤ 10 | 16–24 | 5 |
| 920 DU 20 | 152–172 | 118–143 | ≤ 25 | 5–9 | 5 |
| 920 DU 40 | 168–178 | 121–131 | ≤ 17 | 10–16 | 5 |
| 909 DU 80 | 172–187 | 118–128 | ≤ 10 | 18–24 | 5 |
| 920 DU 80 | 177–192 | 121–131 | ≤ 14 | 18–24 | 5 |
| 950 DU 80 | 188–200 | 136–146 | ≤ 12 | 18–24 | 5 |
| 093 DU 120 | 186–201 | 119–129 | ≤ 6.5 | 28–38 | 5 |
| 951 DU 120 | 191–206 | 131–141 | ≤ 9 | 28–38 | 5 |
| 930 DU 120 | 189–204 | 117–127 | ≤ 6,5 | 28–38 | 5 |
| 920 DU 120 | 191–203 | 118–128 | ≤ 14 | 28–38 | 5 |
| 980 DU 100 | 211–231 | 167–182 | ≤ 14 | 20–30 | 5 |

**New product:**

| | | | | | |
|---|---|---|---|---|---|
| HP92 DU 80 | 180–200 | 116–126 | ≤ 20 | 20–30 | 5 |

### Product information

- DU = Dry powder of unexpanded Expancel® Microspheres
- Delivered in FIBC 500 kg, or in fibre drums net weight 50 kg.
- Use the product within three years after production date, if unopened.
- Not all grades available in all locations. Check local sales office for availability.

Expancel®